Numerical Approaches about the Morphological Description Parameters for the Manganese Deposits on the Magnesite Ore Surface

Mehmet Bayirli and Tuba Ozbey

Physics Department, Science and Literature Faculty, Balikesir University, Cagis, 10145, Balikesir, Turkey

Reprint requests to M. B.; E-mail: mbayirli@balikesir.edu.tr

Z. Naturforsch. **68a,** 405 – 411 (2013) / DOI: 10.5560/ZNA.2013-0010
Received October 5, 2012 / revised December 20, 2012 / published online May 22, 2013

Black deposits usually found at the surface of magnesite ore or limestone as well as red deposits in quartz veins are named as natural manganese dendrites. According to their geometrical structures, they may take variable fractal shapes. The characteristic origins of these morphologies have rarely been studied by means of numerical analyses. Hence, digital images of magnesite ore are taken from its surface with a scanner. These images are then converted to binary images in the form of 8 bits, bitmap format. As a next step, the morphological description parameters of manganese dendrites are computed by the way of scaling methods such as occupied fractions, fractal dimensions, divergent ratios, and critical exponents of scaling. The fractal dimension and the scaling range are made dependent on the fraction of the particles. Morphological description parameters can be determined according to the geometrical evaluation of the natural manganese dendrites which are formed independently from the process. The formation of manganese dendrites may also explain the stochastic selected process in the nature. These results therefore may be useful to understand the deposits in quartz vein parameters in geophysics.

Key words: Crystal Structure of Minerals; Numerical Methods; Critical Exponents; Structure of Disordered Solids.
PACS numbers: 91.60.Ed; 02.60-x; 64.60.F-; 61.43.Hv

1. Introduction

Various morphologies may be found in nature which carry the name as dense structures, elongated finger arrays, forests of trees, dendrites, and islands [1]. One such structure are manganese dendrites (MnDs) that form at the surface of magnesite ore [2], rock agates [1, 3], and limestones [4, 5]. MnDs tend to raise much theoretical interest [3, 4]. Due to their common occurrence, detailed knowledge of the genetic conditions of the MnDs can be of great practical interest in understanding geological environments. Nevertheless, geologists tend to consider them as rather meaningless structures in deciphering geological environments. The reason of that may probably be due to the uncertainty of their genesis and their formation mechanism [4, 6].

The formation mechanism and the structure of MnDs are yet unknown and still under discussion. The formation of MnDs can be explained as stochastic selected process in nature. MnDs consist of manganese oxide (MnO_2 and Mn_2O_3) and iron oxide (Fe_2O_3). They are usually named incorrectly as 'pseudo-fossils' that are formed as naturally occurring fissures along fractures at the surface and/or interface of magnesite ore or rocks that are filled by percolating mineral solutions [1, 6]. They have a visible form in two dimensions and are found in the joint surfaces in sedimentary rocks. The size of individual MnDs ranges from about 0.5 cm to about 20 cm in length. A three-dimensional form of dendrites develops in fissures in quartz and form moss agate [7]. MnDs are often explained on the basis of diffusion-limited aggregation (DLA) [8], reaction-diffusion aggregation (RDA) [5], and experimental studies [6]. For example, a previous study at the surface of magnesite ore revealed the presence of several morphologies that vary from dendrites to compact morphologies [2]. They were determined as seven different groups due to the geometrical structures and the values of critical exponents of the correlation functions and the fractal dimensions [2, 7]. In a different study,

MnDs have been determined in nine different groups using the results of the fractal and shapes analyses on vein quartz in one dimension [7].

The fractal dimension is a parameter that quantifies the roughness of the pattern surface. This value can be used to characterize the geometrical complexity of bounded sub-patterns and pattern groups. Its value does not take an integer value. The fractal dimension for MnDs has been described in many works [1 – 7]. However, it has not been fully characterized in the morphological structure of the patterns because the visually distinct patterns may have similar values of fractal dimension. Unfortunately, there are very few studies regarding the scaling critical exponents for the macro internal structures and their characterization of the perimeter–area relation in the literature for MnDs. Moreover, scaling properties that describe the structures of MnDs into morphologies can be studied quantitatively using power-law treatments.

Scaling and self-similarity are imported concepts in modern statistical physics. They are determined especially in morphological phase transitions for both natural and experimental patterns. Scaling is generally described by a simple power law consisting of exponents, irrespective of experimental and natural details such as the formation condition of patterns and specific experimental systems [9]. The natural formation pattern for the same surface, which is a kind of phase transition, exhibit scaling and self-similar properties insensitive to formation details. This is one reason why scaling treatments are chosen to analyze both the experimental and natural results [9, 10].

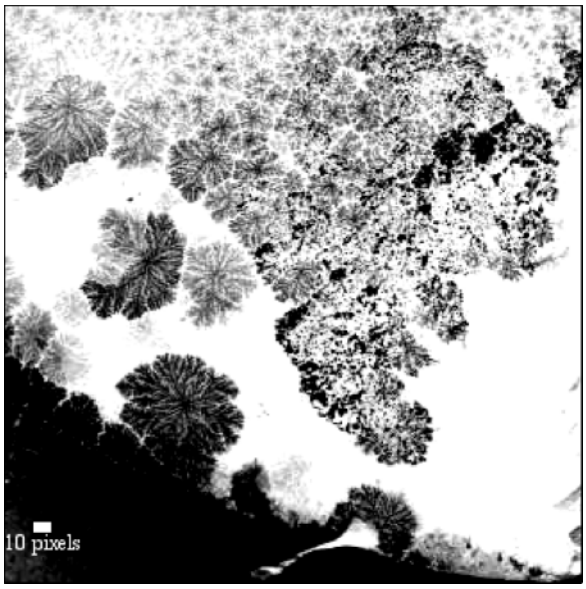

Fig. 1. Typical image of natural MnDs formed on magnesite ore. It has an interface which MnDs form from the interface toward the surface [2].

Scaling method and fractal geometry are also determined as useful concepts for the analyses of complex and irregular structures. Both concepts are based on the image analysis methods which involve forming a grid surface in square lattices of a given image with patterns. For that purpose, the fractal dimensions, the occupied fractions, the perimeter–area relationships, and the scaling exponents along joint planes for all islands that show MnDs patterns at the surfaces of the magnesite ore have been determined. The divergent ratios and the characteristic lengths are also computed. Our results can be useful to compare similar experimental finding such as nickel–phosphorus and MnDs patterns on vein quartz in one dimension.

2. Scaling Method

First of all, the surface of the magnesite ore showing MnDs patterns is scanned by a scanner (Epson Stylus DX485). A typical image of such MnDs is shown in Figure 1. The MnDs pattern morphologies, which have changed from dendrites to compact structures, are distributed randomly at the surface of the magnesite ore. With the high contrast, the black dendrites can be clearly differentiated from the white vein magnesite ore in the images. From the sample, four different regions are selected according to visible morphological structure. They are shown in Figure 2. These are labeled as MnDs-A, MnDs-B, MnDs-C, and MnDs-D. There are compact patterns in MnDs-A, semi compact and dendrites in MnDs-B, dendrites patterns in MnDs-C, and interface pattern in MnDs-D. These images were transferred to a computer for analysis. In order to differentiate these samples, they are filtered by Gaussian blur $\sigma = 2$ and then converted in the BMP format. Such an image containing 216 144 six-digit numbers is considered as an intensity image type and represents an 512-by-512 array of 8-bits integers that are linearly scaled to produce a white and black colour map.

3. Results and Discussion

Numeric computations are performed on a finite square lattice of $L = 512$ pixels by the scaling method.

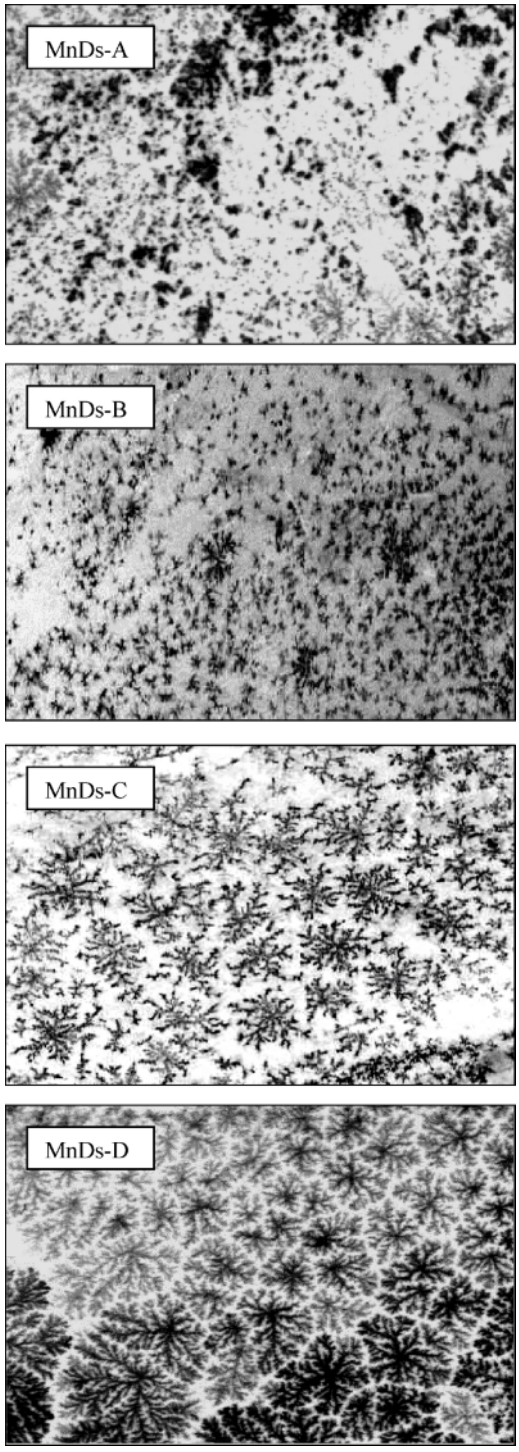

Fig. 2. Square-selection scanning images of the natural MnDs. The dark regions are MnDs and bright regions are magnesite ore.

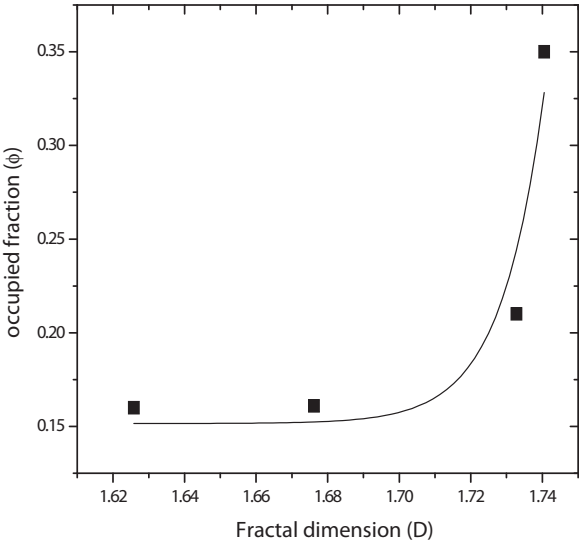

Fig. 3. Occupied fraction $\phi(N,L)$ as a function of the fractal dimension D for MnDs patterns.

The length of square MnDs particles is chosen to be the unit of length. The occupied fraction $\phi(N,L)$ of the particle flux of the magnesite ore surface is given as

$$\phi(N,L) = NL^{-d}, \tag{1}$$

where N is the total number of particles, and d is the Euclidian dimension. The numbers of particles N are computed as 41 993, 42 385, 55 111, and 93 690 and the occupied fractions $\phi(N,L)$ are computed as 0.160, 0.162, 0.210, and 0.357 for the MnDs patterns in $d = 2$, respectively. There are several different patterns in the images: 402 in MnDs-A, 274 in MnDs-B, 107 in MnDs-C, and 96 in MnDs-D at the surface of the magnesite ore.

The fractal dimensions are an index of scale dependent on the MnDs surface and may be described with different concepts. They are defined as the similarity dimension for the self-similarity patterns, the mass dimension for the constant density Euclidean patterns, the Haussdorff–Besicovitch dimension for the bounded sets and subsets, and capacity dimension of the pattern and/or pattern groups [1, 3, 4]. The similarity dimension is meaningful only for exactly self-similar patterns [11, 12]. However, some MnDs patterns are both self-similarity and non-self-similar patterns which can be described as a part of percolation patterns [1, 3, 4].

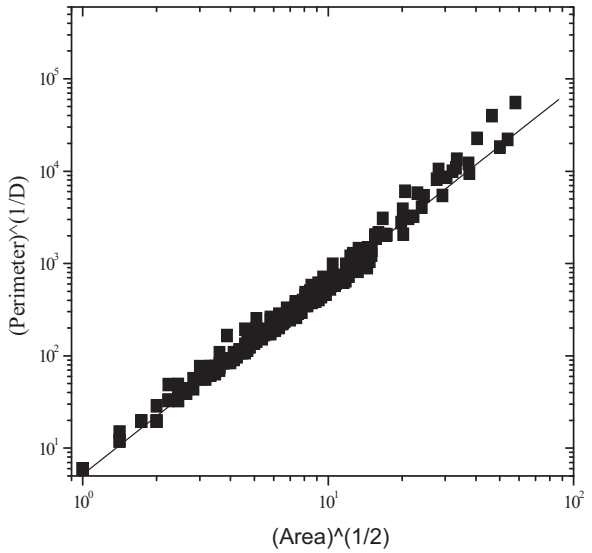

Fig. 4. Perimeter–area relation for MnDs-A. The value of the strain line slope is about 2.092.

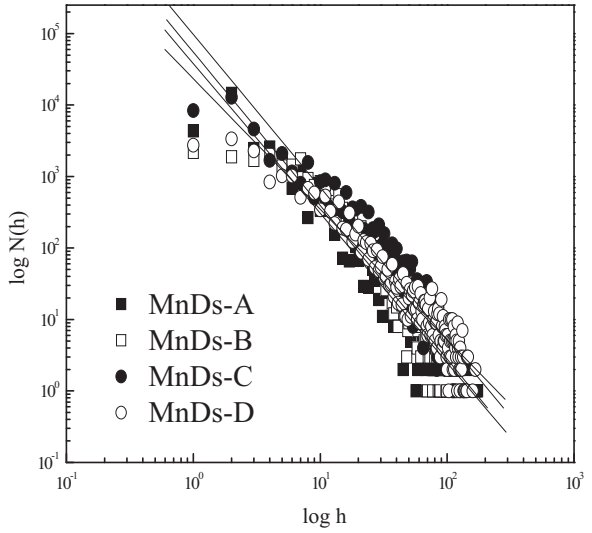

Fig. 5. Typical log–log plot of h vs. $N(h)$. The slopes of the straight lines fitted to data change yield scaling exponents from 2.092 to 1.825.

The MnDs that grow randomly and take various geometrical structures have too many subsets. Moreover, the islands in the subsets are found to be separated from each other with various distances. In general, MnDs patterns are often replaced by box dimension or capacity at the surface of the magnesite ore. A δ-cover of A is a summation of patterns of diameters which contains any bounded union of sub-MnDs pattern area A at the square lattice surface and a minimum linear dimension $\delta > 0$. Furthermore, each sub-pattern of diameter δ ingrained in the grid surface on the off-square lattice is composed of a combination of particles of the MnDs. When the limit exists, we donate by $N_\delta(A)$ the smallest number of patterns in a δ-cover of A and describe the box dimension D of A as

$$D = \lim_{\delta \to 0} \frac{\log N_\delta(A)}{\log(1/\delta)}. \tag{2}$$

The box dimension can be thought for measuring how well a set can be covered with small boxes of equal size because the limit remains unchanged if $N_\delta(A)$ is replaced by the smallest number of E-dimensional square areas of the sides δ needed to cover A, or even the number of areas of a δ lattice that intersect A [11, 12]. The fractal dimensions for them are estimated using the box-counting method [1, 3]. In this method, $N(A)$ is the number of boxes or squares needed to cover entire patterns on the magnesite ore, and δ is the size of the boxes. The estimation of fractal dimension D involves step-by-step iteration. δ is increased and $N(A)$ is computed for each step. The steps for the box size used in this study follow $\delta = 2^0, 2^1, 2^2, \ldots$ pixels. A plot of $\log N(A)$ versus $\log \delta$ is made for the pattern data sets. This relation is linear, and the absolute value of the slope corresponds to the fractal

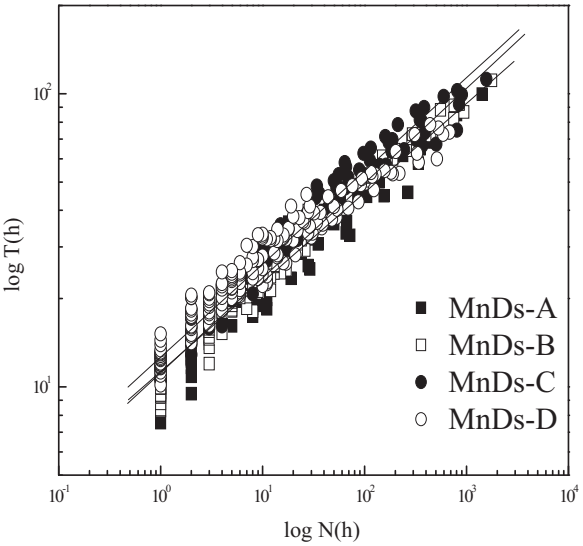

Fig. 6. Typical log–log plot of $N(h)$ vs. $T(h)$. The slopes of the straight lines fitted to data changes range from 0.304 to 0.278.

Table 1. Result values of the occupied fraction, fractal dimension, perimeter-area exponents, and critical exponents α and β of the scaling.

	Occupied Fraction (ϕ)	Box-Counting (D)	SIM (γ)	Divergent Ratio (ρ_D)	α	β
MnDs-A	0.160	1.626 ± 0.013	1.614 ± 0.012	2.092 ± 0.016	2.092 ± 0.065	0.304 ± 0.007
MnDs-B	0.161	1.676 ± 0.018	1.581 ± 0.010	2.151 ± 0.014	2.147 ± 0.073	0.323 ± 0.005
MnDs-C	0.210	1.732 ± 0.067	1.465 ± 0.015	1.228 ± 0.012	2.136 ± 0.068	0.317 ± 0.005
MnDs-D	0.350	1.740 ± 0.045	1.513 ± 0.006	1.317 ± 0.005	1.825 ± 0.050	0.278 ± 0.005

dimension D of the pattern [2–4, 7, 10]. They have a narrow range from 1.626 to 1.740, and the average value is 1.75. The values of fractal dimension are reported as 1.78 on limestone [5] and 1.51 for MnDs on quartz in one dimension [7]. It is also reported as 1.69 between two laminae of fine-grained calcarenite from a flysh facies [6]. Dendrite patterns with broad and short branches have generally bigger values of fractal dimension compared to those with long and thin branches [4, 6].

To determine the influence of the occupied fraction on the fractal dimension, we plotted the occupied fraction $\phi(N,L)$ of the samples as a function of the fractal dimension D. Figure 3 shows the occupied fraction $\phi(N,L)$ as a function of the fractal dimension D.

The relationship between $\phi(N,L)$ and D can be computed by numerical analyses. The initial parameter estimate function $\phi(D)$ using the nonlinear exponential decay regression method is taken in variant form (as seen in (3)) given by

$$\phi = \phi_0 + A\,\mathrm{e}^{(-D/t_1)}, \tag{3}$$

where A and t_1 are the correlation parameters. These parameters are obtained from $\phi(N,L)$ and D by searching for the fit on all regions of aggregations. The correlation parameters are computed as $\phi_0 = 0.151 \pm 0.030$, $A = 1.182\mathrm{E}-64 \pm 1.462\mathrm{E}-62$, and $t_1 = -0.012 \pm 0.010$. The coefficient r^2 of nonlinear regression is computed as 0.92517.

In nature, each pattern group with standard planar shapes can be geometrically similar. Nevertheless, they can be found in different sizes. Yet they may have a characteristic length and critical exponent. The critical exponent of every MnDs is computed using the slit-island method (SIM) which was proposed by Mandelbrot et al. [11]. They applied the method first to a set of 'islands' obtained by the two-dimensional cuts of broken metal surfaces. SIM involves selecting surface patterns with a plane at a given height. Thus, different island-like areas at each surface appear for both the different height values and the critical exponents.

Analyses of perimeter–area data from patterns on the magnesite ore confirm the existence of a perimeter–area power-law relationship,

$$A(\delta) = C_1 P(\delta)^{\gamma}, \tag{4}$$

where C_1 is the intercept on the A-axes, δ is the yardstick value, and γ is the slope of the $\log A - \log P$ plots as the critical exponent [13]. The constant C_1 which appears in (4) is estimated by performing a linear regression on the log perimeter–log area data. This is shown in Figure 4. From this analysis, slopes that range from 1.614 to 1.465 for the patterns of the MnDs groups are computed.

The divergent ratio ρ_D for the fractal patterns in two dimensions is in correlation with the perimeter and the square root of enclosed area for the patterns. It is independent of the size of the particles for the patterns of the same geometrical structure. The values of the divergent ratio ρ_D are 3.44 for circles, 4.00 for squares, and 4.56 for triangles, respectively [11, 13]. Its values increase with the complexity and angularity of the pattern of the outline. Nevertheless, the perimeter of patterns depends on the scale of measurement. Mandelbrot also proposed for the fractal curves using the length of yardstick δ the divergent ratio

$$\rho_D = C_2 P(\delta)^{1/D} A(\delta)^{-(1/2)}, \tag{5}$$

where C_2, P, and A are a constant, the perimeter, and the area, respectively. δ is a yardstick value and it is taken as one pixel. The divergent ratio is independent of the size of fractal patterns but depends on the yardstick according to the scaling parameters. The divergent ratio ranges from 2.092 to 1.228 for the four different samples. The relationship between the shape of the dendrite and the divergent ratio compared to the divergent ratio for the MnDs patterns is shown more clearly. A simple dendrite on magnesite ore with broad

branches has the bigger fractal divergent ratio. The values decrease when the branch thickness slim for the MnDs patterns. The values of the divergent ratio ρ_D are reported for the manganese dendrites on vein quartz which have different geometrical structures ranging from 0.840 to 0.830 in one dimension [7].

Moreover, the critical exponents of the scaling [14, 15] are also examined in the four selected regions possessing various morphologies in two dimensions at the surface of the magnesite ore. All square-sectional images were digitized in linear dimensions with a resolution of 512×512 pixels and were transformed into 8 bits binary images. The root-mean-square (RMS) thickness and the number of pixels that lie within a thickness of h is defined by

$$T(h) = \left\langle x_i - \langle x_i \rangle \right\rangle^{\frac{1}{2}}, \tag{6}$$

where $\langle \ldots \rangle$ indicates an average over the number of pixels of h, and x_i is the thickness of pixel i. In addition, the values h can be taken as 1, 2,$\ldots nx_i$, and n is an integer. Equation (6) represents the number of accumulative pixels that lie under a thickness of h changing in a range from 0 to 512 in units of pixels,

$$N(h) = \sum_{x \le h} \rho(x_i), \tag{7}$$

where $\rho(x_i)$ is the particle density and it is defined as

$$\rho(x_i) = \begin{cases} 1 \text{ if a dark pixel exists at } x_i, \\ 0 \text{ if a bright pixel exists at } x_i. \end{cases} \tag{8}$$

In (8), $\rho(x_i)$ is defined as 0 if a bright pixel exits at x_i, 1 if a dark pixel exits at x_i. The relationship between $N(h)$ and h is defined by

$$N(h) \propto h^{-\alpha}, \tag{9}$$

and the relationship between $T(h)$ and h is defined by

$$T(h) \propto N(h)^{\beta}, \tag{10}$$

where α and β are the critical exponents of the scaling for the morphological structures. The values of the critical exponents α and β in Figure 5 and 6 are estimated to 2.136 and 0.317, respectively, using the linear regression method, which yields $\alpha\beta = 0.635$ for the four different pattern groups. As the exponent α decreases with the occupied fraction, reversely the exponent β increases. As particles in the pattern groups accumulate in pixels, this consequently leads to a $T(h) \propto h$ term. These results and their 95% confidence limits for the four images are also summarized in Table 1.

Figure 5 shows that when $x_i \to h$ increases, the $N(x_i)$ value decreases for the MnDs patterns. It also implies that the distribution of the accumulated pixels, which are particles, is determined only by h. Their RMS values $T(h)$ increase as power of $N(h)$ as in the case of the DLA model for computer simulation growth at a two-dimensional surface on the basis of parameters $\alpha = 1.70$ and $\beta = 0.41$. They have been reported according to the occupied fraction and the number of the pattern sites [14]. The critical exponents α and β are reported to be 1.15 and 0.91, respectively, by Saito and Okudaira for the macro internal structure of porous nickel–phosphorus films using the electro-deposition method [15]. Our results are greater than Saito's and Okudaira's results.

4. Conclusion

In this paper, the morphological description parameters are computed by using the scaling method for the natural manganese dendrites. According to their geometrical structures, they may have different sizes. They may be formed along joint surfaces at the magnesite ore, limestones or in a quartz vein. The island groups of the patterns can be characterized computing the occupied fraction, the fractal geometry, and the scaling exponents for the pattern groups on a square lattice using the scaling method. The fractal dimensions of the MnDs are estimated using box-counting algorithm and SIM algorithm change. The first method produced a result ranging from 1.626 to 1.740, whereas the second method produced a result ranging from 1.614 to 1.465. Our results confirm that the structural characteristics of MnDs form DLA processes and determine the multi-dimensionality of the space in which the growth process occurs. They also confirm that structural characteristics of MnDs are insensitive to features such as surface curvatures.

Meanwhile, these results determine the morphological transitions of the natural mineral dendrites independent of the formation process. The growth formation of MnDs may also explain the stochastic selected processes such as DLA. These results can prove to be useful for geophysics and the earth sciences.

[1] A. L. Barbarasi and H. E. Stanley, Fractal Concepts in Surface Growth, Cambridge University Press, Cambridge 1995.
[2] M. Bayirli, Physica A: Stat. Mech. Appl. **353**, 1 (2005).
[3] P. Meakin, Fractals, Scaling and Growth Far From Equilibrium, Cambridge University, Press, Cambridge 1998.
[4] T. Vicsek, Fractal Growth Phenomena, Word Scientific, Singapore 1992.
[5] B. Chopard, H. C. Herrmann, and T. Vicsek, Nature 353, 409 (1991).
[6] J. M. García-Ruiz, F. Otálora, A. Sanchez-Navas, and F. Higes-Rolando, The Formation of Manganese Dendrites as the Material Record of Flow Structures, in 'Fractals and Dynamics Systems in Geosciences', Ed. J. H. Kruhl, Springer, Berlin 1994, pp. 307–318.
[7] T. F. Ng and G. H. The, Geol. Soc. Malay. **55**, 73 (2009).
[8] T. A. Witten and L. M. Sender, Phys. Rev. Lett. **27**, 5786 (1983).
[9] J. Los, P. Bennema, P. H. J. van Dam, W. J. P. van Enckevort, F. A. Hollander, and C. N. M. Keulemans, J. Phys.-Condens. Mat. **12**, 3195 (2000).
[10] M. Bayirli and H. Kockar, Z. Naturforsch **65a**, 777 (2010).
[11] B. B. Mandelbrot, D. E. Passaja, and A. J. Paullay, Nature, 308 (1984).
[12] B. B. Mandelbrot, The Fractal Geometry of Nature, Freeman, New York 1983.
[13] E. M. Schlueter, R. W. Zimmerman, P. A. Witherspoon, and N. G. Cook, Eng. Geol. **48**, 199 (1997).
[14] P. Meakin, Phys. Rev. A **27**, 2616 (1983).
[15] M. Saitou and Y. Okudaira, J. Electrochem. Soc. **151**, C674 (2004).